Check for updates

How to cite: *Angew. Chem. Int. Ed.* **2023**, *62*, e202307059
doi.org/10.1002/anie.202307059

Helical Polymers | Hot Paper

Conformational Kinetics in Chiral Poly(diphenylacetylene)s: A Dynamic *P/M* Memory Effect

*Juan José Tarrío, Rafael Rodríguez, Jeanne Crassous, Emilio Quiñoá, and Félix Freire**

Abstract: Dynamic *P*/*M* (*plus*/*minus*) helical memory in chiral dissymmetric poly(diphenylacetylene)s (PDPA) is shown using a PDPA that bears the benzamide of (*L*)-alanine methyl ester as pendant. For a single chiral polymer, it is possible to obtain either *P* or *M* helical structures in a specific solvent without the presence of any chiral external stimuli. To do that, it is necessary to combine the conformational control at the pendant group with a high steric hindrance at the backbone. In this case, by thermal annealing in low-polar solvents, an *anti*-conformer is stabilized at the pendant which commands a *P* helix in the PDPA. Next, solvent removal followed by addition of a polar solvent such as dimethyl sulfoxide (DMSO), results in the kinetic conformationally trapped *P* helix. However, in this medium, the preferred handedness and the thermodynamic macromolecular helix for poly-(*L*)-**1** is *M*. This process also occurs in the opposite way. Electronic circular dichroism (ECD) and circularly polarized luminescence (CPL) studies show that the dynamic memory effect is present both in ground and excited states.

Introduction

Dynamic helical polymers play an important role in the chemistry of materials due to their application in different fields such as asymmetric catalysis,[1–6] chiral recognition,[7] sensing,[8–14] photoelectronic devices[15–18] or biological media.[19] This fact is related to the helical structure[20,21] adopted by the polymer—*P* or *M* helix, compressed/stretched—, which can be tuned by the presence of external stimuli, and to the functional groups present in the pendant that will be oriented in a certain position towards the helix. Thus, it is possible to do helix inversion, screw sense enhancement or stretching/compression of the helix through different mechanisms—supramolecular interactions,[22–28] solvent polarity,[29–31] sergeants and soldiers effect,[26,33] majority rules[26] or chiral-to chiral communication mechanisms[33–35]—that follow a cooperative effect. These structural changes in dynamic helical polymers are usually triggered either by the conformational composition of a chiral pendant or by the establishment of a supramolecular interaction between achiral pendants and chiral molecules. In the later system, Yashima and co-workers found that, in some cases, when the chiral additive is removed from the solution, the dynamic helical polymer, i.e., a poly(pheylacetylene) (PPA) bearing a carboxylic acid at the para position, maintain the helical structure induced by the chiral additive.[14,36–37] This phenomenon was denoted as "memory effect".[38] They found that this process can be extrapolated to other polyacetylene derivatives, such as poly(biphenylacetylene)s (PBPA)[39–40] and poly(diphenylacetylene)s (PDPAs).[41–42] These systems were recently denoted as first- (PPAs), second- (PBPAs) and third- (PDPAs) generation of static helicity memory respectively. In these polymers the helix induction provoked by addition of a chiral additive can be preserved after complete removal of the nonracemic guest.[38] Interestingly, Maeda and co-workers demonstrated that in achiral PDPAs the memorized *P* or *M* helical structure induced by supramolecular interaction with chiral molecules is retained after post-functionalization with a chiral molecule.[42–43]

Herein, we want to go a step forward and explore the helical memory in chiral dynamic helical polymers, where the chiral group responsible of the induction of the helical sense is present in the monomer repeating unit and therefore, covalently linked to the polymer main chain. Our objective is to prepare a helical polymer that shows dynamic *P*/*M* macromolecular helicity memory, where the helical sense control is achieved by altering the conformational composition at the pendant group, while the steric hindrance at the backbone is responsible of the memory effect. The large energy barrier to switch between the *P*/*M* helices results in the emergence of a memory effect which can be thermodynamically controlled. To perform these studies, we chose PDPAs as dynamic helical polymers. This family of helical polymers has attracted the attention of the scientific community lately due to the properties associated with the PDPA backbone, such as chemical, photochemical, and

[*] Dr. J. J. Tarrío, Dr. R. Rodríguez, Prof. E. Quiñoá, Prof. F. Freire
Centro Singular de investigación en Química Biolóxica e Materiais Moleculares (CiQUS) and Departamento de Química Orgánica, Universidade de Santiago de Compostela
15782 Santiago de Compostela (Spain)
E-mail: felix.freire@usc.es
Dr. R. Rodríguez, Dr. J. Crassous
ISCR (Institut des Sciences Chimiques de Rennes), Univ Rennes, CNRS
UMR 6226, 35000 Rennes (France)

© 2023 The Authors. Angewandte Chemie International Edition published by Wiley-VCH GmbH. This is an open access article under the terms of the Creative Commons Attribution Non-Commercial License, which permits use, distribution and reproduction in any medium, provided the original work is properly cited and is not used for commercial purposes.

© 2023 The Authors. Angewandte Chemie International Edition published by Wiley-VCH GmbH

thermal stabilities, combined with their intrinsic optical and chiroptical properties–CD, fluorescence emission, CPL–, which make PDPAs promising materials. Originally, these materials were considered as static, although recently it was found possible to modulate the elongation or helical sense of chiral PDPAs demonstrating the dynamic properties of these polymers.[44–50]

Results and Discussion

Our group reported a chiral PDPA that shows a solvent-dependent helix inversion achieved based either on the polar/non-polar or the donor/non-donor character of the solvent.[49] In these studies, the polymer adopts a preferred helical sense after thermal annealing at high temperature (e.g. 80 °C during 24 h) in a specific solvent.[48–53] One of these PDPAs, poly-(*L*)-**1**, a dissymmetric chiral poly(diphenylacetylene) that bears the benzamide of (*L*)-alanine methyl ester at one of the aryl rings of the diphenylacetylene was reported by our group.[48] This polymer was prepared according to the protocol reported by Tang and co-workers.[55] The number average molar mass (M_n) and molar mass dispersity (M_w/M_n) of poly-**1** were 1.4×10^4 and 1.43 respectively, as determined by gel permeation chromatography (GPC) using THF as eluent and polystyrene narrow standards (PSS) as calibrants.

From a previous study we found that *M* or *P* helical senses can be induced in the polyene backbone of poly-(*L*)-**1** after thermal annealing (80 °C/24 h) in donor (dimethylformamide (DMF), DMSO) and non-donor ($CHCl_3$, MeCN) solvents respectively (Figure 1a).[48] This different screw sense excess obtained in donor and non-donor solvents is associated to a conformational change at the pendant group, which was monitored by VCD studies (Figure 1c–d). Thus, while in donor solvents, the carbonyls of the amide and ester groups are *synperiplanar* oriented (*syn* conformation), in non-donor solvents these two groups are *antiperiplanar* oriented (*anti* conformation) (Figure 1c). As a result, a chiroptical and circularly polarized luminescence (CPL) switch was obtained (Figure 1b).[48]

The large energy barrier between the two helical orientations (*P* and *M*) of poly-(*L*)-**1** is consequence of the intrinsic steric hindrance found in the PDPA backbone and therefore, a dynamic helical memory for poly-(*L*)-**1** is expected. To demonstrate this hypothesis a *M* helical sense was first induced in poly-(*L*)-**1** by thermal annealing in a donor solvent ($ECD_{400\,nm}>0$ in DMSO) (Figure 2a–b). Next, the solvent was removed under reduced pressure and a non-donor solvent was added (i.e., $CHCl_3$, Figure 2a). The ECD trace remains virtually identical to the one obtained in donor solvents ($ECD_{400\,nm}>0$) (Figure 2a–b) demonstrating the presence of a memory effect in chiral PDPAs. Analogous experiments were also done in the opposite direction, 1) thermal annealing of poly-(*L*)-**1** in a non-donor solvent ($CHCl_3$)—*P* helix induction, $ECD_{400\,nm}<0$—, 2) solvent removal and 3) addition of a donor solvent (DMSO), which produces a practically identical ECD trace ($ECD_{400\,nm}<0$) (Figure 2a–b). These studies demonstrate that the memory

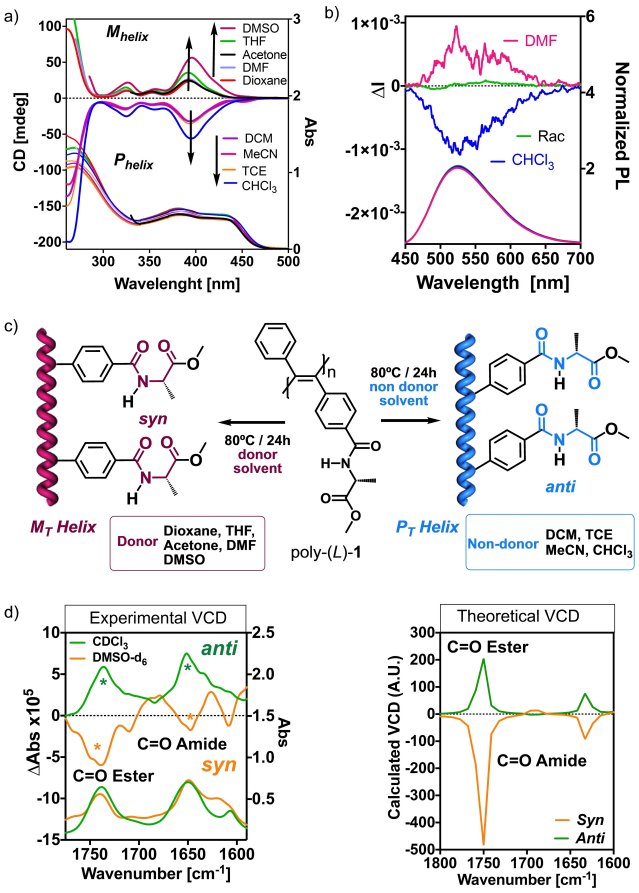

Figure 1. a) ECD and UV spectra of poly-(*L*)-**1** in different solvents (0.5 mg/mL, 1 mm path). b) CPL spectra of poly-(*L*)-**1** ($\lambda_{Exc}=365$ nm, 0.3 mg/mL). c) Schematic illustration of the solvent-triggered conformational change in the pendant group that promotes the helix inversion after a thermal annealing. d) Experimental and theoretical VCD studies of poly-(*L*)-**1** in DMSO and $CDCl_3$. [poly-(L)-**1**] = 0.5 mg/mL.

effect in chiral PDPAs works in both directions, resulting in a remarkable dynamic memory effect.

Additionally, the CPL properties gained during the thermal annealing of the PDPA are retained once redissolved in a solvent with different donor character (Figure 2c). Consequently, the dynamic memory effect is observed both in the ground and the excited states.

Next, we proceed to analyze the extension of the memory effect through thermodynamic studies. Thus, time dependent ECD experiments were carried out for the memorized *P* and *M* helical structures for poly-(*L*)-**1**. A *P* helix was induced in poly-(*L*)-**1** in $CHCl_3$ after thermal annealing at 80 °C—thermodynamic structure, P_T—. Then a conformational kinetically trapped *P* helix is formed by solvent removal followed by addition of DMSO (P_{CKT}). This solution was then heated up to 80 °C and ECD measurements were recorded every 6 minutes during 948 min to study the evolution of a *P* memorized helix—kinetically trapped structure, P_{CKT}—towards an M_T one—thermodynamic structure, M_T—(Figure 3a,b) where a complete helix inversion is produced after 16 h, indicating a high energy

© 2023 The Authors. Angewandte Chemie International Edition published by Wiley-VCH GmbH

15213773, 2023, 32, Downloaded from https://onlinelibrary.wiley.com/doi/10.1002/anie.202307059 by Universidade de Santiago de Compostela, Wiley Online Library on [31/10/2023]. See the Terms and Conditions (https://onlinelibrary.wiley.com/terms-and-conditions) on Wiley Online Library for rules of use; OA articles are governed by the applicable Creative Commons License

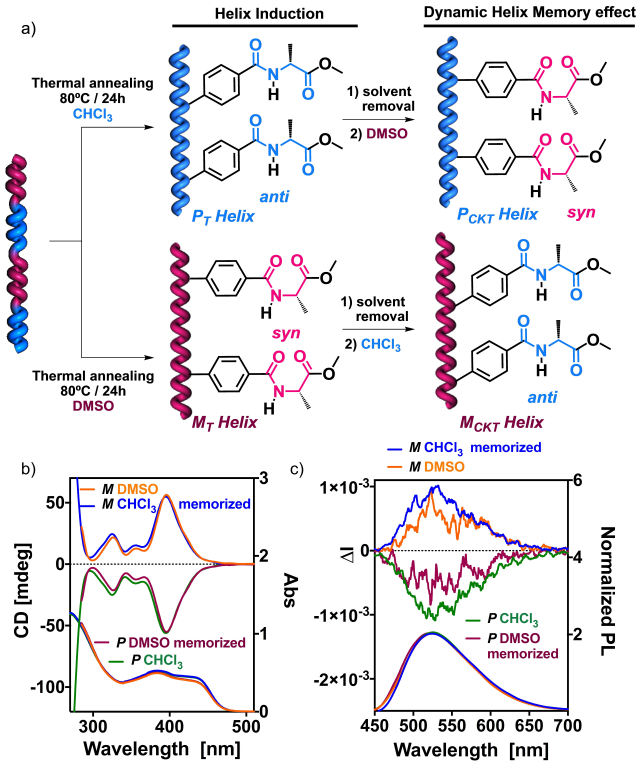

Figure 2. a) Schematic illustration of the *P*/*M* helix induction of poly-(*L*)-**1** after thermal annealing and its dynamic memory effect. b) ECD and c) CPL studies showing the dynamic memory effect of poly-(*L*)-**1**. [poly-(*L*)-**1**] = 0.5 mg/mL, λ_{Exc} = 365 nm.

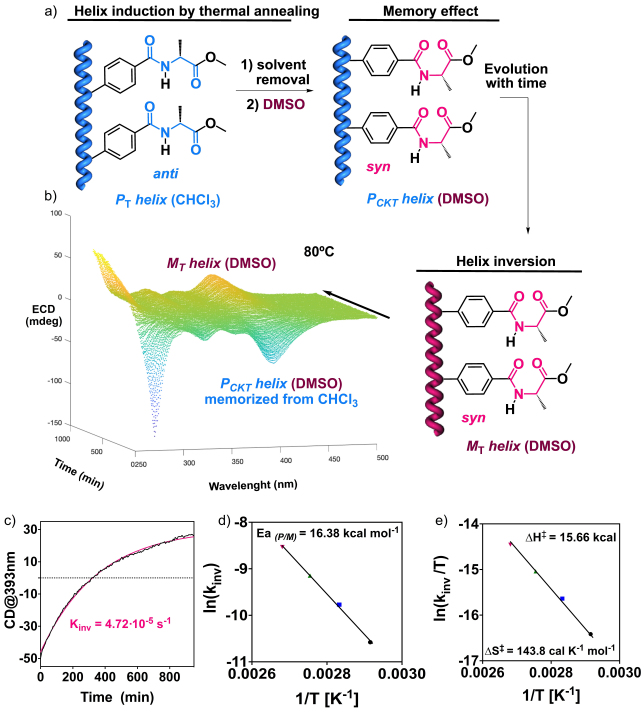

Figure 3. a) Schematic illustration of the helix inversion produced with time from a memorized helix of poly-(*L*)-**1**. (b-c) Time dependent ECD studies for a DMSO solution of poly-(*L*)-**1** at 80 °C pre-annealed in $CHCl_3$. d) Arrhenius plot of $\ln(k_{inv\ P/M})$ obtained from the slope of c) versus $T^{-1}K^{-1}$. e) Eyring plot of $\ln(k_{inv\ P/M}/T)$ vs $T^{-1}K^{-1}$.

barrier for the helix inversion process. To gauge the different kinetic and thermodynamic parameters of this process, the variation of the ECD at 393 nm vs time was plotted and fitted to equation (1):

$$ECD = ECD_0 + (Plateau - ECD_0) \cdot (1 - e^{(-K_{inv} \cdot t)}) \quad (1)$$

Where ECD_0 is the value of the ECD signal when time is zero and Plateau is the ECD value at infinite times.

In this case, the equation obtained is:

$$ECD = -46.02 + (76.81) \cdot (1 - e^{(-0.002834 \cdot t)}) \quad (2)$$

From this equation, the kinetic constant for the helix inversion process from P_{CKT} to M_T ($k_{inv\ P/M}$) for poly-(*L*)-**1** in DMSO at 80 °C is $k_{inv\ P/M} = 2.83 \cdot 10^{-3}\ min^{-1}$ ($k_{inv\ P/M} = 4.72 \cdot 10^{-5}\ s^{-1}$) (Figure 3c). Similar studies were carried out at different temperatures: 70°, 90° and 100 °C. The $k_{inv\ P/M}$ decreases at 70 °C when compared to that obtained at 80 °C ($k_{inv\ P/M\ (70°C)} = 2.60 \cdot 10^{-5}\ s^{-1}$), while it increases when the experiment is performed at higher temperature ($k_{inv\ P/M\ (90°C)} = 9.76 \cdot 10^{-5}\ s^{-1}$, $k_{inv\ P/M\ (100°C)} = 1.73 \cdot 10^{-4}\ s^{-1}$) (see Figure S7). The values of the $k_{inv\ P/M}$ at different temperatures were used to calculate the activation energy barrier (E_a) of the helix inversion by plotting $\ln(k_{inv\ P/M})$ vs $T^{-1}K^{-1}$ (Figure 3d) and fitting them to the Arrehnius equation (3).

$$k_{inv\ P/M} = A \cdot e^{\left(\frac{-E_a}{RT}\right)} \quad (3)$$

The activation energy barrier to produce a *P* to *M* helix inversion of poly-(*L*)-**1** is $E_{a\ (P/M)} = 16.38\ kcal\ mol^{-1}$. In addition, by applying the Eyring equation (4) —$\ln(k_{inv}/T)$ vs $T^{-1}K^{-1}$—, the thermodynamic parameters $\Delta H^{\ddagger}$ and $\Delta S^{\ddagger}$ for the helical inversion were calculated. In this case, $\Delta H^{\ddagger} = 15.66\ kcal\ mol^{-1}$ and $\Delta S^{\ddagger} = 143.8\ cal\ K^{-1}\ mol^{-1}$, (Figure 3e).

$$\ln\frac{K}{T} = -\frac{\Delta H^{\ddagger}}{RT} + \ln\frac{k_B}{h} - \frac{\Delta S^{\ddagger}}{R} \quad (4)$$

Analogous studies were carried out for the opposite helix inversion process from M_{CKT} to P_T. 1,1,2,2-tetrachloroethane (TCE) was chosen as solvent to induce an M_{CKT} due to its high boiling point compared to $CHCl_3$. Thus, poly-(*L*)-**1** adopts a M_{CKT} helix in TCE, which evolves towards a P_T helix by thermal annealing at 80 °C (see SI). From these studies it was possible to obtain a similar kinetic inversion constant ($K_{inv\ M/P} = 4.83 \cdot 10^{-5}\ s^{-1}$), the activation energy barrier to produce a *M* to *P* helix inversion ($E_{a(M/P)} = 16.42\ kcal\ mol^{-1}$) and thermodynamic parameters $\Delta H^{\ddagger} = 15.71\ kcal\ mol^{-1}$ and $\Delta S^{\ddagger} = 143.1\ cal\ K^{-1}\ mol^{-1}$, demonstrating the reversibility of the process (see Figure S8).

Finally, the duration of the memory effect was analyzed by monitoring the evolution of the conformational kinetically trapped structures of poly-(*L*)-**1** [P_{CKT} in DMSO and M_{CKT} in $CHCl_3$] towards the corresponding thermodynamic

© 2023 The Authors. Angewandte Chemie International Edition published by Wiley-VCH GmbH

15213773, 2023, 32, Downloaded from https://onlinelibrary.wiley.com/doi/10.1002/anie.202307059 by Universidade de Santiago de Compostela, Wiley Online Library on [31/10/2023]. See the Terms and Conditions (https://onlinelibrary.wiley.com/terms-and-conditions) on Wiley Online Library for rules of use; OA articles are governed by the applicable Creative Commons License

ones (M_T in DMSO and P_T in $CHCl_3$) at room and lower temperatures (i.e., 4 °C and −20 °C). These studies showed that, when a solution of poly-**1** containing the conformational kinetically trapped structure is stored at low temperature, a longer-lasted memory effect is obtained. For instance, a decrease of 20 % in the ECD trace is observed after 2 days at room temperature, while at 4 °C and −20 °C a decrease of just 4 % and 2 %, respectively, is observed. A screw sense excess of the conformational kinetically trapped structure is still observed after several months (See Figure S10).

Conclusion

In conclusion, in this work it is demonstrated, through an illustrative example, that chiral PDPAs show a dynamic *P*/*M* memory effect, where conformational kinetically trapped and thermodynamic structures with opposite macroscopic chiralities (*P*/*M*) can be selectively isolated in any polymer solution, independently on the solvent used to dissolve the polymer. For instance, while a thermodynamic P_T structure is obtained for poly-(*L*)-**1** after thermal annealing at 80 °C in $CHCl_3$, this macromolecular scaffold can be stored as a conformational kinetically trapped structure in DMSO (P_{CKT}) although the thermodynamic scaffold in this solvent is the opposite (M_T). The lasting-memory effect depends on the solution temperature and goes from hours to months. Importantly, this process is reversible, and a M_T structure obtained for poly-(*L*)-**1** can be kinetically trapped in $CHCl_3$ (M_{CKT}), although the thermodynamic structure in this solvent is a *P* helix (P_T). The different kinetic and thermodynamic parameters involved in this process were extracted from time and temperature dependent ECD studies. Remarkably, not only the helical structure is memorized, but also other properties associated with the helical scaffold, such as CPL emission. This is the first time to our knowledge that a chiral helical polymer shows memory effect through a combination of conformational control at the pendant group together with the high helix inversion energy barrier in PDPAs. By taking advantage of this phenomenon the two *P* or *M* screw senses can be obtained for poly-(*L*)-**1** in any solvent, opening a new horizon in the application of these materials.

Acknowledgements

We thank financial support from AEI (PID2019-109733GB-I00) and Juan de la Cierva Incorporación contract (IJC2020-042689-I, R. R.). Xunta de Galicia (ED431C 2022/21, Centro Singular de Investigación de Galicia acreditación 2019–2022, ED431G 2019/03 and the European Regional Development Fund (ERDF) are gratefully acknowledged. J. J. T. thanks MICINN for an FPU contract.

Conflict of Interest

The authors declare no conflict of interest.

Data Availability Statement

The data that support the findings of this study are available in the supplementary material of this article.

Keywords: Chiral Polymers · Circular Dichroism · Conformational Kinetics · Helices · Memory Effect

[1] M. Ando, R. Ishidate, T. Ikai, K. Maeda, E. Yashima, *J. Polym. Sci. Part A* **2019**, *57*, 2481–2490.
[2] C. Zhang, Y. Qiu, S. Bo, F. Wang, Y. Wang, L. Liu, Y. Zhou, H. Niu, H. Dong, T. Satoh, *J. Polym. Sci. Part A* **2019**, *57*, 1024–1031.
[3] R. P. Megens, G. Roelfes, *Chem. Eur. J.* **2011**, *17*, 8514–8523.
[4] S. Ikeda, R. Takeda, T. Fujie, N. Ariki, Y. Nagata, M. Suginome, *Chem. Sci.* **2021**, *12*, 8811–8816.
[5] Y. Nagata, R. Takeda, M. Suginome, *ACS Cent. Sci.* **2019**, *5*, 1235–1240.
[6] T. Ikai, M. Ando, M. Ito, R. Ishidate, N. Suzuki, K. Maeda, E. Yashima, *J. Am. Chem. Soc.* **2021**, *143*, 12725–12735.
[7] E. Anger, H. Iida, T. Yamaguchi, K. Hayashi, D. Kumano, J. Crassous, N. Vanthuyne, C. Roussel, E. Yashima, *Polym. Chem.* **2014**, *5*, 4909–4914.
[8] R. Rodríguez, E. Rivadulla-Cendal, M. Fernández-Míguez, B. Fernández, E. Quiñoá, F. Freire, *Angew. Chem. Int. Ed.* **2022**, *61*, e202209953.
[9] K. Maeda, D. Hirose, N. Okoshi, K. Shimomura, Y. Wada, T. Ikai, S. Kanoh, E. Yashima, *J. Am. Chem. Soc.* **2018**, *140*, 3270–3276.
[10] R. Sakai, E. B. Barasa, N. Sakai, S. I. Sato, T. Satoh, T. Kakuchi, *Macromolecules* **2012**, *45*, 8221–8227.
[11] E. Yashima, K. Maeda, *Macromolecules* **2008**, *41*, 3–12.
[12] K. Maeda, E. Yashima, *Supramol. Chirality* **2006**, 47–88.
[13] R. Nonokawa, E. Yashima, *J. Am. Chem. Soc.* **2003**, *125*, 1278–1283.
[14] E. Yashima, K. Maeda, Y. Okamoto, *Nature* **1999**, *399*, 449–451.
[15] Y. Gao, F. Guo, P. Cao, J. Liu, D. Li, J. Wu, N. Wang, Y. Su, Y. Zhao, *ACS Nano* **2020**, *14*, 3442–3450.
[16] H. L. Park, J. Jun, M. H. Kim, S. H. Lee, *Org. Electron.* **2022**, *100*, 106385.
[17] Z. G. Zheng, Y. Q. Lu, Q. Li, *Adv. Mater.* **2020**, *32*, 1905318.
[18] C. Sa, X. Xu, X. Wu, J. Chen, C. Zuo, X. Fang, *J. Mater. Chem. C* **2019**, *7*, 13097–13103.
[19] T. Leigh, P. Fernandez-Trillo, *Nat. Chem. Rev.* **2020**, *4*, 291–310.
[20] E. Yashima, N. Ousaka, D. Taura, K. Shimomura, T. Ikai, K. Maeda, *Chem. Rev.* **2016**, *116*, 13752–13990.
[21] E. Yashima, K. Maeda, H. Iida, Y. Furusho, K. Nagai, *Chem. Rev.* **2009**, *109*, 6102–6211.
[22] K. Y. Kim, J. Kim, C. J. Moon, J. Liu, S. S. Lee, M. Y. Choi, C. Feng, J. H. Jung, *Angew. Chem. Int. Ed.* **2019**, *58*, 11709–11714.
[23] X. Guan, S. Wang, G. Shi, J. Zhang, X. Wan, *Macromolecules* **2021**, *54*, 4592–4600.
[24] J. Qiao, S. Lin, J. Li, J. Tian, J. Guo, *Chem. Commun.* **2019**, *55*, 14590–14593.
[25] R. Ishidate, T. Sato, T. Ikai, S. Kanoh, E. Yashima, K. Maeda, *Polym. Chem.* **2019**, *10*, 6260–6268.

© 2023 The Authors. Angewandte Chemie International Edition published by Wiley-VCH GmbH

15213773, 2023, 32, Downloaded from https://onlinelibrary.wiley.com/doi/10.1002/anie.202307059 by Universidade de Santiago de Compostela, Wiley Online Library on [31/10/2023]. See the Terms and Conditions (https://onlinelibrary.wiley.com/terms-and-conditions) on Wiley Online Library for rules of use; OA articles are governed by the applicable Creative Commons License

[26] R. Ishidate, A. J. Markvoort, K. Maeda, E. Yashima, *J. Am. Chem. Soc.* **2019**, *141*, 7605–7614.
[27] K. Shimomura, T. Ikai, S. Kanoh, E. Yashima, K. Maeda, *Nat. Chem.* **2014**, *6*, 429–434.
[28] S. Leiras, E. Suárez-Picado, E. Quiñoá, R. Riguera, F. Freire, *Giant* **2021**, *7*, 100068.
[29] S. Leiras, F. Freire, J. M. Seco, E. Quiñoá, R. Riguera, *Chem. Sci.* **2013**, *4*, 2735–2743.
[30] R. Rodríguez, E. Quiñoá, R. Riguera, F. Freire, *Small* **2019**, *15*, 1970070.
[31] R. Rodríguez, E. Suárez-Picado, E. Quiñoá, R. Riguera, F. Freire, *Angew. Chem. Int. Ed.* **2020**, *59*, 8616–8622.
[32] J. Bergueiro, F. Freire, E. P. Wendler, J. M. Seco, E. Quiñoá, R. Riguera, *Chem. Sci.* **2014**, *5*, 2170–2176.
[33] K. Cobos, R. Rodríguez, E. Quiñoá, R. Riguera, F. Freire, *Angew. Chem. Int. Ed.* **2020**, *59*, 23724–23730.
[34] M. Alzubi, S. Arias, R. Rodríguez, E. Quiñoá, R. Riguera, F. Freire, *Angew. Chem. Int. Ed.* **2019**, *131*, 13499–13503.
[35] K. Cobos, E. Quiñoá, R. Riguera, F. Freire, *J. Am. Chem. Soc.* **2018**, *140*, 12239–12246.
[36] C. I. Simionescu, V. Percec, S. Dumitrescu, *J. Polym. Sci. Polym. Chem. Ed.* **1977**, *15*, 2497–2509.
[37] V. Percec, J. G. Rudick, M. Peterca, P. A. Heiney, *J. Am. Chem. Soc.* **2008**, *130*, 7503–7508.
[38] E. Yashima, K. Maeda, *Bull. Chem. Soc. Jpn.* **2021**, *94*, 2637–2661.
[39] T. Ikai, S. Takeda, E. Yashima, *ACS Macro Lett.* **2022**, *11*, 525–531.
[40] M. Fukuda, M. Morikawa, D. Hirose, T. Tsuyoshi, T. Nishimura, E. Yashima, K. Maeda, *Angew. Chem. Int. Ed.* **2023**, *62*, e202217020.
[41] S. Sona, D. Hirose, Y. Kurihara, K. Maeda, *J. Mater. Chem. C* **2023**, *11*, 1271–1277.
[42] K. Maeda, M. Nozaki, K. Hashimoto, K. Shimomura, D. Hirose, T. Nishimura, G. Watanabe, E. Yashima, *J. Am. Chem. Soc.* **2020**, *142*, 7668–7682.
[43] D. Hirose, K. Ogino, K. Uematsu, K. Maeda, *J. Chromatogr. A* **2022**, *1675*, 463164.
[44] D. Hirose, M. Nozaki, M. Maruta, K. Maeda, *Chirality* **2022**, *34*, 597–608.
[45] S. Sueyoshi, T. Taniguchi, S. Tanaka, H. Asakawa, T. Nishimura, K. Maeda, *J. Am. Chem. Soc.* **2021**, *143*, 16136–16146.
[46] A. Yurtsever, S. Das, T. Nishimura, R. Rodríguez, D. Hirose, K. Miyata, A. Sumino, T. Fukuma, K. Maeda, *Chem. Commun.* **2021**, *57*, 12266–12269.
[47] K. Maeda, D. Hirose, M. Nozaki, Y. Shimizu, T. Mori, K. Yamanaka, K. Ogino, T. Nishimura, T. Taniguchi, M. Moro, E. Yashima, *Sci. Adv.* **2021**, *7*, eabg5381.
[48] J. J. Tarrío, R. Rodríguez, B. Fernández, E. Quiñoá, F. Freire, *Angew. Chem. Int. Ed.* **2022**, *61*, e202115070.
[49] Y. J. Jin, K. U. Seo, Y. G. Choi, M. Teraguchi, T. Aoki, G. Kwak, *Macromolecules* **2017**, *50*, 6433–6438.
[50] J. J. Tarrío, B. Fernández, E. Quiñoá, F. Freire, *J. Mater. Chem. C* **2023**, *11*, 8378–8382.
[51] K. U. Seo, Y. J. Jin, H. Kim, T. Sakaguchi, G. Kwak, *Macromolecules* **2018**, *51*, 34–41.
[52] C. K. W. Jim, J. W. Y. Lam, C. W. T. Leung, A. Qin, F. Mahtab, B. Z. Tang, *Macromolecules* **2011**, *44*, 2427–2437.
[53] H. Kim, K. U. Seo, Y. J. Jin, C. L. Lee, M. Teraguchi, T. Kaneko, T. Aoki, G. Kwak, *ACS Macro Lett.* **2016**, *5*, 622–625.
[54] X. A. Zhang, A. Qin, L. Tong, H. Zhao, Q. Zhao, J. Z. Sun, B. Z. Tang, *ACS Macro Lett.* **2012**, *1*, 75–79.
[55] X. Wang, H. Hu, W. Wang, A. Qin, J. Z. Sun, B. Z. Tang, *Polym. Chem.* **2015**, *6*, 7958–7963.

Manuscript received: May 19, 2023
Accepted manuscript online: June 20, 2023
Version of record online: July 3, 2023

© 2023 The Authors. Angewandte Chemie International Edition published by Wiley-VCH GmbH

15213773, 2023, 32, Downloaded from https://onlinelibrary.wiley.com/doi/10.1002/anie.202307059 by Universidade de Santiago de Compostela, Wiley Online Library on [31/10/2023]. See the Terms and Conditions (https://onlinelibrary.wiley.com/terms-and-conditions) on Wiley Online Library for rules of use; OA articles are governed by the applicable Creative Commons License